ACS APPLIED MATERIALS & INTERFACES

Research Article

www.acsami.org

Water-Assisted Growth of Uniform 100 mm Diameter SWCNT Arrays

Roman M. Wyss,[†] Jennifer E. Klare,[‡] Hyung Gyu Park,[†] Aleksandr Noy,[§] Olgica Bakajin,*[,‡] and Valentin Lulevich*[,‡]

[†]Nanoscience for Energy Technology and Sustainability, Department of Mechanical and Process Engineering, ETH Zurich, Sonneggstrasse 3, Zürich CH-8092, Switzerland

[‡]Porifera Inc., 3502 Breakwater Court, Hayward, California 94545, United States

[§]Physical and Life Sciences Directorate, Lawrence Livermore National Laboratory, Livermore, California 94550, United States

Supporting Information

ABSTRACT: We report a simple method for growing high-quality single-walled carbon nanotube (SWCNT) arrays on 100 mm wafers via the addition of water vapor to highly purified gases during the CNT growth step. We show that adding a small amount of water during growth helps to create a uniform catalyst distribution and yields high-quality (Raman G/D of 26 ± 3), high-density (up to 6×10^{11} cm^{-2}) and uniform SWCNT arrays on 100 mm large wafers. We rationalize our finding by suggesting that the addition of water decreases catalyst mobility, preventing its coarsening at higher temperatures. We also report a new mechanism of catalyst inactivation in wafer-scale growth using ultrapurified gas sources by the formation of large, 5 ± 3 μm iron particles. We found such formations to be common for substrates with large temperature gradients, such as for wafers processed in a typical cold-wall chemical vapor deposition reactor.

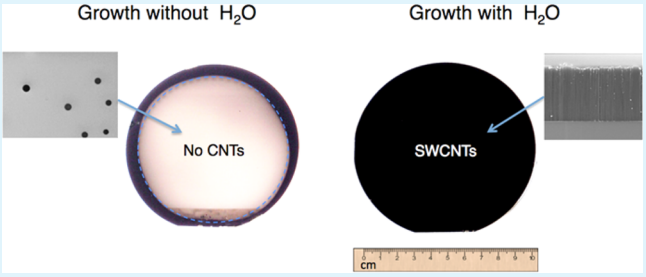

KEYWORDS: *aligned SWCNT array, wafer scale CNT synthesis, water assisted SWCNT growth, catalyst ripening, catalyst mobility, catalyst inactivation*

1. INTRODUCTION

Carbon nanotube (CNT) membranes have unique smooth hydrophobic CNT pores that serve as perfect frictionless conduits, in which gas and fluid flows can be many orders of magnitude higher than in conventional pores of the same size.[1,2] Well-established carbon chemistry allows for relatively simple CNT pore functionalization, which creates a selective membrane while maintaining high transport rates through the pores.[3,4] A significant effort has been expended in scaling up carbon nanotube membranes for chemical separations,[5] selective electroosmotic pumping,[6] and drug delivery.[7] Because recent measurements of ion transport and mobility in CNT membranes suggest that only small-diameter high-quality nanotubes contribute to flow enhancements in CNT pores,[6] synthesis of high-quality CNTs is required to realize the full potential of this technology. Unfortunately, reliable production of sub-2 nm diameter, high-quality and uniform CNT arrays on a wafer scale, as required for the fabrication of the high-performance CNT membranes, still presents a challenge.

Numerous studies[8−10] have demonstrated synthesis of excellent quality single-walled CNTs (SWCNTs) with well-controlled diameters on substrates up to 1 cm in diameter. However, while growth of aligned MWCNTs has previously been scaled to 4 and 8 in. wafers in 2005 and 2008,[11] respectively, there are relatively few papers reporting the synthesis of the high-density well-graphitized aligned SWCNT films on large substrates. This rarity is largely associated with problems around uniform catalyst deposition and activation, which are greatly amplified in a large-scale chemical vapor deposition (CVD) reactor.[9,12,13] Differences in reactor design and the extreme sensitivity of CNT synthesis to ppm levels of impurities make it difficult to scale up, reproduce, and compare the known methods for aligned CNT synthesis.[14] Plasma-enhanced chemical vapor deposition (PECVD) usually improves the array uniformity. However, it drastically decreases the quality of CNTs because unlike the thermal CVD,[15] it does not allow for the fine control of the reaction mixture chemical composition. Crucially, CNTs produced by PECVD are too large in diameter for the CNT membrane application: the smallest reported diameter for high-quality (Raman G/D ratio around 20) CNT arrays produced by PECVD is only 4−5 nm.[16]

Water assisted growth and its strong effect on CNT quality and yield were first reported by Hata et al.[12] It is well-established that water extends the lifetime of the catalyst and thus enables the synthesis of millimeter-tall SWCNTs.[17] Water also increases the growth window and the catalyst tolerance to variations in the process gas composition.[18] Further, its been shown that addition H_2O[9], CO_2[19,20] and other oxygen containing enhancers[21] can improve growth by cleaning off

Received: August 30, 2014
Accepted: November 19, 2014
Published: November 19, 2014

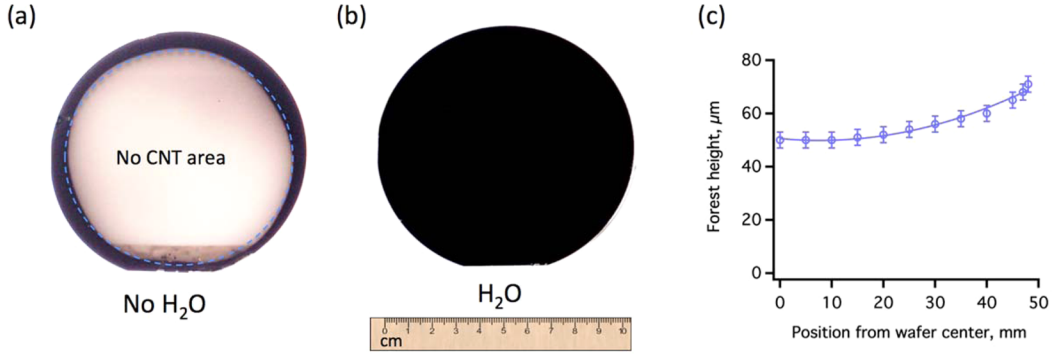

Figure 1. 100 mm wide wafer with vertically aligned CNTs grown at 725 °C (a). The typical pattern showing a large "no growth" area is visible in the center of the wafer. (b) Similar wafer with CNT's grown using addition of small amount of water. Forest height radial distribution on typical 100 mm wafer is shown in panel c. Scale bar for wafers is shown on the bottom.

amorphous carbon coating that deactivates catalyst. It has also been suggested that water not only reactivates the catalyst by removing the carbon coating but also inhibits Oswald ripening. This reduces the ripening rate, thus extending lifetime of the catalyst and producing a uniform SWCNT forest.[22,23]

In this paper, we demonstrate that when we use ultrapurified gas sources without the addition of water, the iron catalyst forms large micrometer-sized particles that do not catalyze CNT growth. The addition of a small amount of water to highly purified gases during the CNT growth step results in arrays of high-quality aligned CNTs with uniform quality across 100 mm wide substrates. Crucially, we reveal evidence for a previously unreported effect of water on the initial catalyst particle formation by inhibiting not only Oswald but also Smoluchowski[24] ripening. We suggest that water prevents large particle formation by oxidizing the iron and increasing the interaction between the catalyst and the substrate, therefore eliminating large catalyst denuded zones. Specifically, water increases the temperature at which micrometer particle formation occurs, allowing for CNT synthesis within a larger temperature window, which, in turn, results in better nanotube wall graphitization and ultimately better array quality on large area substrates.

2. MATERIALS AND METHODS

2.1. Catalyst Preparation and Catalytic CVD. The 0.5 nm thick Fe catalyst was deposited by e-beam evaporation (SC 1000, Semicore, Livermore, CA) on a 30 nm thick Al_2O_3 support on a standard test grade Si wafer (Ultrasill Inc., Hayward CA). E-beam deposition of Fe and Al_2O_3 films was conducted at a chamber pressure in the range of $1-2.0 \times 10^{-6}$ mbar at a deposition rate of 0.1 nm/s. The CNT growth was carried out in a vertical cold-wall CVD reactor (Black Magic, Aixtron, Cambridge, UK). After the chamber was cleaned with oxygen plasma, the catalyst substrate was loaded on the sample stage at a substrate temperature above 200 °C to avoid moisture condensation, and the chamber was evacuated below 0.2 mbar. First, the sample was annealed at 500 °C for 10 min in hydrogen atmosphere at 15 mbar. Then, it was quickly (at a ramp rate of 300 °C min^{-1}) heated to 725 °C in the H_2 atmosphere at 90 mbar. A CNT growth step began by adding 5 sccm of the C_2H_2 gas to 700 sccm of H_2. All the process gases were purified using gas purifiers (SAES Pure Gas Inc., San Luis Obispo, CA) to reduce impurities such as acetone, H_2O and O_2 to the ppb level. Water was added into the gas mixture by bubbling 10–15 sccm of Ar through a chilled (10 °C) bubbler. The water content in the final gas mixture was monitored by an Easidew hydrometer (Michell Instruments, Cambridge, UK) with accuracy of approximately 100 ppm_v, installed at the showerhead inlet of the CVD reactor. "Water grown" samples in this work refer to addition of 300–400 ppm_v of moisture as measured by a hygrometer installed at the showerhead inlet.

2.2. Structural Characterization of SWCNT Forests. As-grown CNTs were characterized using scanning electron microscopy (SEM, Zeiss ULTRA 55 at 5 keV), transmission electron microscopy (JEOL 2100-F FETEM at 120 keV) and Raman spectroscopy (ARAMIS Microscope, Horiba Inc., Japan) with a 532 nm laser line. All Raman spectra were taken with a 50× objective lens.

The height of the SWCNT forest was determined by averaging five or more height measurements taken along the fresh cut, cross-sectional edge of the sample using SEM. Samples for the TEM analysis were prepared by sonicating vertically grown CNTs in 10 mL of isopropyl alcohol (98%, Aldrich) and collecting the suspension on a lacey carbon TEM grid (Ted Pella, Inc.). All data in this work is presented as "mean ± standard deviation".

The density of the CNT forest was as determined using the mass gain of the wafer, mass of a single 2 nm diameter SWCNT from Futaba et al.[8] and the diameter and number of walls determined by TEM.

2.3. Atomic Force Microscopy (AFM) and X-ray Photoelectron Spectroscopy (XPS) Analyses of Ultrathin Fe Catalysts. Surface topography and roughness of the as-deposited and annealed catalyst substrates was analyzed with MFP-3D AFM (Asylum Research, Santa Barbara, CA) operating in the tapping mode with a scan rate of 0.5–1 Hz. A supersharp silicon tip from Nanosensor (Neuchatel, Switzerland) with the resonance frequency of 300 kHz and the stiffness of 43 N/m was used to acquire the AFM scan data. The topography was measured in ambient conditions in tapping mode. For alumina roughness measurements AFM images with a size of 250 × 250 nm were taken at three different spots on each sample. A plane was subtracted from each image to remove the sample tilt and set the lowest point of an image to zero.

X-ray photoelectron spectroscopy (XPS) was performed at the Molecular Foundry at Lawrence Berkeley National Laboratories using a PHI 5400 XPS analyzer. The XPS was performed in ultra-high-vacuum conditions (2×10^{-7} Pa base pressure) with monochromatic Mg Kα (1253.6 eV) radiation. The spectrometer energy scale was calibrated using adventitious carbon. The elemental composition was determined using AugerScan from RBD Enterprises.

3. RESULTS AND DISCUSSION

Vertical cold-wall CVD reactors are designed to achieve uniform material deposition over large areas. However, because certain degrees of variations in the temperature and reaction mixture composition over a large (ca. 100 mm) area are somehow inevitable, the product uniformity depends highly on the stability of the growth process over a relatively wide parametric window. Unfortunately, CNT growth is known to be extremely sensitive to the fairly minute variations in the process parameters. Thus, it was not surprising when our initial

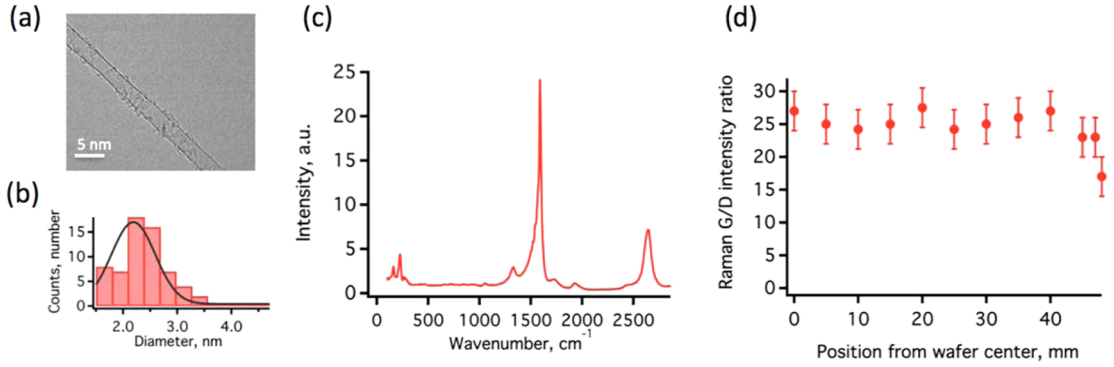

Figure 2. TEM images of a SWCNT produced by water-assisted growth (a) and CNT diameter distribution from the wafer-size sample (b). Typical Raman spectrum of water-assisted wafer scale array shown on (c). Raman intensity is normalized to D peak value. Typical Raman G/D peak intensity radial distribution on 100 mm wafer is shown in panel d.

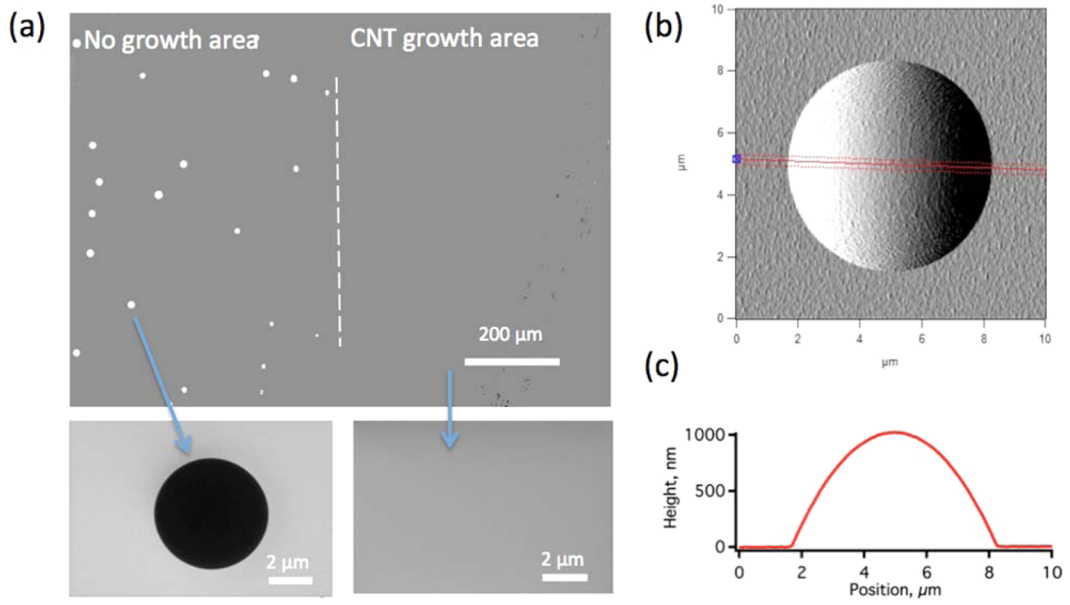

Figure 3. (a) Optical image of the boundary between no-growth and CNT grow areas on wafer processed at 725 °C. SEM zoom-in into both areas is shown below. AFM of typical surface of large catalyst particle is shown in panel b and corresponding cross-section in panel c.

attempts to grow high-quality SWCNTs on 100 mm diameter silicon wafers at temperatures as high as 725−750 °C, which are required for single- and double-walled CNT synthesis using acetylene, revealed a pattern formation issue persistently: CNTs did not grow on significant portions of the wafer (Figure 1a). The size of this no-growth area was not dependent on acetylene or hydrogen partial pressures, or overall chamber pressure during synthesis. At lower temperatures (650−675 °C) used in a MWCNT growth, these no-growth areas did not occur or were significantly smaller. Because some residual CNTs grew on the wafer edges during the high-temperature runs, we postulate that the preferential edge growth is the result of lower temperature at the wafer edges (in the cold wall CVD reactors, such as used in this work, the temperature of the wafer on the edges is always lower than the middle due to radiation heat losses and nonuniform temperature distribution in the reactor itself[25]). We also note that such no-growth defects are less pronounced on smaller substrates within the very same reactor, where temperature inhomogeneity is much smaller. These observations point to a general issue: at higher temperatures that are required for the growth of high-quality SWCNT arrays the yield of CVD growth on large-scale substrates falls dramatically.

In contrast, the addition of Ar containing 300−400 ppm_v of moisture (as measured by a hygrometer installed at the showerhead inlet) to the process gases resulted in good CNT growth across the entire wafer (Figure 1b). The increase in array height at the edge of the wafer is attributed to variation in the substrate temperature and reaction composition mixture that is typical for a cold wall reactor,[25] see Figure 1c. We note that variation in catalyst and alumina thickness cannot be responsible for observed radial height uniformity because they are deposited in a 9-wafer e-beam evaporator that produces only linear thickness gradients. With a 725 °C growth temperature, using 0.5 nm thick iron catalysts, our setup typically produced a SWCNT forest with a diameter of 2.1 ± 0.6 nm (Figure 2a,b) and a Raman G/D ratio of 26 ± 3. Significantly, these quality parameters were consistent across the wafer, see Raman G/D ratio distribution in Figure 2d. SEM forest cross-section, TEM of individual tubes and tube diameter distribution from different spots on typical wafer are shown in the Supporting Information, Figures S2 and S3. The average mass gain for a wafer (78 cm^2) was 26 mg for a 100 μm tall

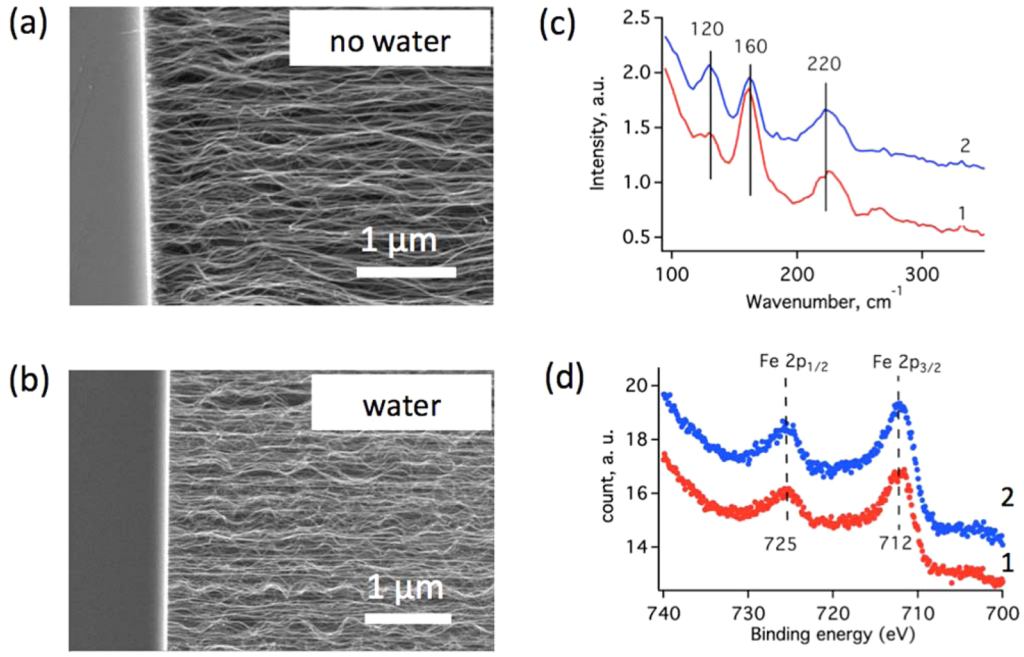

Figure 4. SEM images of CNTs grown on 0.5 nm iron catalyst without water (a) and with small amount of water (b). Raman spectra of control (curve 1, red) and water-assisted growth (curve 2, blue) in RBM region (c). XPS spectra of control (curve 1, red) and water treated catalyst (curve 2, blue) shown in panel d.

forest. Using the mass of a single 2 nm diameter SWCNT from Futaba et al.,[8] we estimate the CNT density to be 6.4×10^{11} cm^{-2}, typical for the CVD-grown high-quality CNT arrays.[9,10] This high density suggests that for water-assisted wafer-sized CNT synthesis, the majority of the catalyst remains active during the growth process and yields high-quality nanotubes. We note that there is only a finite window where water has a beneficial effect: the addition of larger amounts of water (600–700 ppm_v) results in no CNT growth.

To investigate why water-assisted growth eliminated the "bad CNT growth" area, we examined the boundary between the good growth and the no-growth areas. To clearly see this boundary without interference from CNTs, we performed a control CNT growth run without the carbon source (acetylene). Optical microscopy of the catalyst of the no-growth area revealed formation of shiny microscopic particles, not visible in normal growth area (Figure 3a). Higher resolution SEM images of the "good" growth and "bad growth" areas suggest that the particles form only in the "bad growth" area and have a highly symmetric round shape (we also performed a control experiment where we burned CNTs in air for 30 min at 600 °C following a previously reported protocol[26] and found the similar particle formation in no-growth areas but with less clear boundaries). While number and density of these microparticles observed in the no-growth area vary from wafer to wafer, atomic force microscopy (AFM) images reveal that the average diameter and height of the microparticles formed during a 725 °C, 4 min growth on a 100 mm wide wafer measure 5 ± 3 μm and 1 ± 0.3 μm, respectively, which is much larger than typical nanometer-size catalyst particle necessary to nucleate CNTs (Figure 3b,c).

To eliminate the potential influence of temperature inhomogeneity on the growth process, we repeated the experiments in the absence and presence of water moisture on 1 cm^2 wide substrates that should experience rather uniform temperature profiles in our large-scale reactor. On small substrates grown without water at 725 °C, we did not observe any no-growth area or large particle formation, but when we raised the substrate temperature to 750 °C, such microparticles appeared again terminating CNT synthesis. As in the case with synthesis on 100 mm diameter wafers, addition of water was beneficial, preventing the microparticles formation and restoring the CNT growth condition even at 750 °C.

We can also speculate why such dramatic ripening of the catalyst to micrometer-size droplets has not previously been reported in the CNT growth experiments. We note that our system utilized ultrapurified gases that also went through additional scrubber units to remove any oxygen-containing impurities to well below 1 ppb levels.[14] As our experiments suggest, any oxygen-containing impurities are a potent inhibitor of the Fe mobility; thus, by removing these impurities, we were allowing the coarsening process to proceed much further. A similar problem was observed in ultra-high-vacuum silicon nanowires synthesis when all impurities were removed; it turned out that nanowire growth without trace amount of oxygen was terminated earlier due to higher rate of gold diffusion.[27−29] We also note that although the effect of oxygen-containing impurities may seem beneficial, they also contribute to a large extent to the lack of reproducibility and control over the CNT synthesis. Thus, the approach that we present in this work, i.e., removing impurities first and then adding water in a controlled manner independent of the other process gas fluxes, represents a superior way to control the CNT growth process. Indeed, the growth process achieved in our reactor using purified gas sources has a much wider growth parameter "window" than the same reactor using unpurified gas sources

How can a small amount of water vapor affect catalyst ripening and prevent its assembly into large micrometer-size particles? According to CNT catalyst formation theory,[13] the two main factors that control the size of the catalyst particle are iron subsurface diffusion, which decreases the effective particle size, and the ripening process, which increases the particle size.

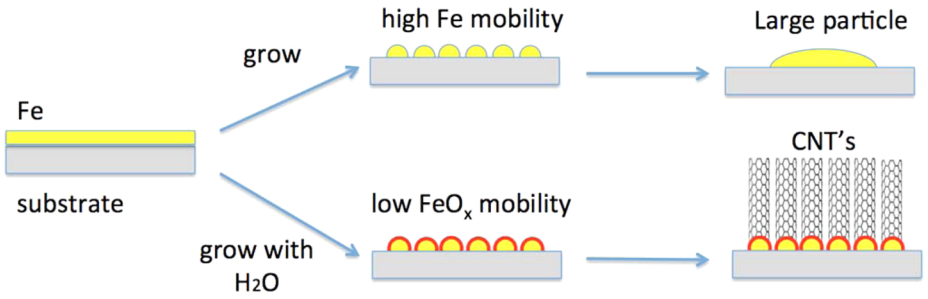

Figure 5. Schematic of the catalyst particle evolution for "no growth" and "water- assisted growth" samples due to different mobility of Fe and FeO_x.

The semispherical shape of the large iron particles and the relatively large 50−300 μm distance between them where no CNT growth was observed suggest that they can form via a coarsening mechanism. The formation of large iron particles that we observed suggests that in this case the ripening represents the dominant process for catalyst inactivation.

In principle, there are two different processes by which coarsening of a surface can occur: Ostwald ripening, when small islands have a vapor pressure greater than large islands, thus creating a net transfer of material from the small to large islands, and Smoluchowski ripening, when coarsening occurs if diffusing islands encounter one another and coalesce into large islands.[24]

It is known that addition of water during CNT synthesis can suppress Ostwald ripening.[22,23] If water suppresses Ostwald ripening in our conditions, then it should stabilize smaller catalyst particles and produce higher CNT forest density with smaller average diameter of CNTs.[30] To investigate this possibility, we synthesized CNTs at 725 °C on 1 cm^2 wide substrates using similar growth recipes with and without addition of water. We also found that growth rates for samples grown with and without water were very similar, 12 ± 4 μm/min and 13 ± 5 μm/min, respectively. High-resolution TEM revealed that the addition of water did not significantly affect the diameter of CNTs: sample grown with water consisted primarily of SWCNT's with a diameter of 2.5 ± 0.8 nm and the control was a mixture of DWCNT and SWCNT's with a diameter of 2.9 ± 1 nm. Raman spectra of both samples have very similar radial breathing mode (RBM) peaks at 120, 160 and 220 cm^{-1} (see inset in Figure 4c) and show very similar G/D ratios: 14−18 for water-assisted growth sample and slightly higher G/D of 15−19 for the control array (see the Supporting Information, Figure S4). Note that on the 1 cm^2 samples, we observed nanotube density and G/D ratio both lower than on the wafer-size substrates, probably because of edge effects and lower actual surface temperatures (temperature of the wafer on the edges is always lower than the middle of the wafer due to radiation heat losses.[25]

As shown in Figure 4a,b, the SWCNTs grown on smaller substrate in the presence of water moisture have higher density compared to the control growth without water. The addition of water actually increased CNT density from $2 \pm 0.5 \times 10^{11}$ cm^{-2} for samples grown without water to $3 \pm 0.5 \times 10^{11}$ cm^{-2} for samples grown with water, as measured using mass gain and the diameter and number of walls determined by TEM. Therefore, we conclude that the suppression of catalyst Oswald ripening by water is one factor in uniform SWCNT growth.

However, Ostwald ripening itself cannot be responsible for the large micron size iron particle formation because forming such extraordinary large islands would take much longer than the time scale of our measurements. On the other hand temperature gradients present in our wafer substrate can significantly alter stochastic island diffusion, making Smoluchowski ripening more likely to be responsible for the observed catalyst coarsening. Thus, we speculate that initial catalyst coarsening during annealing produces small Fe catalyst islands that then rapidly coalesce into much larger droplets via the Smoluchovski ripening. Smoluchovski ripening can be affected in the following two ways: by a change in substrate roughness and by a change in iron particle mobility.[24]

To study if introduction of water changes alumina surface roughness, we used AFM measurements. We prepared two wafers with a layer of alumina and without iron, and performed both water-assisted and control CNT growth runs (without acetylene). The surface roughness of the alumina measured by AFM for these wafers was very similar, 3.4 ± 0.9 nm for the water assisted growth sample and 3.0 ± 0.9 nm for the control sample (see the Supporting Information, Figure S5). The similarity in roughness suggests that the water vapor introduced in CNT growth conditions does not alter the alumina roughness significantly.

The mobility of iron on alumina is known to depend on the oxidation states of iron. Fe^{3+} and Fe^{2+} have much stronger interactions than Fe^0.[31,32] A stronger interaction between the catalyst layer and the substrate reduces the mobility and slows any particle coarsening that may occur. We collected XPS spectra of the catalyst surface processed through standard CNT synthesis run but without adding the acetylene carbon source (Figures 4d and S6, Supporting Information). Typical for an iron catalyst on an alumina substrate,[32−34] the Fe $2p_{3/2}$ peak position (712.0 eV) is shifted from pure Fe (706.8 eV), indicating that the Fe in both samples is fully oxidized to Fe^{3+} and chemically bound to the alumina surface.[32] Unfortunately, XPS peak size and position of both samples are almost identical due to iron oxidation in atmospheric oxygen (although there are known in situ XPS studies[35] using differentially pumped electrostatic lenses attached to reaction cell, performing such experiments was beyond the scope of this work).

However, we can speculate that in the CVD reactor, at substrate temperatures of 700−750 °C where H_2 reduces Fe^{3+} and Fe^{2+} to Fe^0, water vapor added during the growth step oxidizes the iron catalyst, increasing the interaction between alumina and iron oxide and decreasing its mobility. Reduced mobility of iron particles limits the catalyst coarsening via Smoluchowski ripening and prevents the formation of micrometer-size iron particles and catalyst denuded zones, as schematically shown in Figure 5.

Our results suggest that achieving homogeneous arrays of CNT grown on large-area substrates requires a balance between hydrogen-induced iron reduction to highly mobile metallic iron

and water oxidation of iron to less mobile iron oxides. This balance allows for the fine-tuning of iron mobility and, therefore, suppressing both Ostwald and Smoluchowski ripening mechanisms prevents catalyst inactivation over a wider temperature window. This wider optimized process window allows CNT growth on large substrates that are by necessity inhomogeneously heated.

4. CONCLUSIONS

In this paper, we report a simple method of growing high-quality aligned SWCNT arrays on a wafer scale. We show that the addition of water at the beginning of the growth step helps to create uniform catalyst formation even in the presence of finite temperature inhomogeneity. We propose that water suppresses both Ostwald and Smoluchowski catalyst ripening mechanisms, resulting in uniform high-density SWCNT growth and preventing catalyst inactivation over a wider temperature window.

■ ASSOCIATED CONTENT

Supporting Information

Schematic of a the CVD reactor; TEM of individual CNTs, CNT diameter analysis and SEM of CNT forest cross sections for different spots on the water; images of Raman spectra of control and water grown CNT's samples synthesized on small pieces; XPS survey scans of the control sample and the water-assisted growth sample and table with XPS elemental analysis; AFM topography and surface roughness data for water-treated and control catalyst surface. This material is available free of charge via the Internet at http://pubs.acs.org.

■ AUTHOR INFORMATION

Corresponding Authors

*O. Bakajin. E-mail: olgica@poriferanano.com.
*V. Lulevich. E-mail: val.lulevich@poriferanano.com.

Notes

The authors declare no competing financial interest.

■ ACKNOWLEDGMENTS

This work was partially funded by Swiss National Science Foundation (200021-146856). R.M.W. and H.G.P. thank N. Yang, P. Reissner and Prof. A. Stemmer from ETH Zurich for their high-resolution AFM scans. We thank Dr. Virginia Altoe for her help in acquiring SEM, TEM and XPS data. Dr. Ken Teo from Aixtron is acknowledged for his assistance with Black Magic CVD furnace. Work at the Molecular Foundry was supported by the Office of Science, Office of Basic Energy Sciences, of the U.S. Department of Energy under Contract No. DE-AC02-05CH11231. This material is based on work funded by the National Science Foundation under Grant No. IIP-1058572 and by the U.S. Army Research Laboratory and the U.S. Army Research Office under contract/grant number W911NF-09-C-0079. This work was additionally supported by NSF under CMMI-1246804

■ REFERENCES

(1) Holt, J. K.; Park, H. G.; Wang, Y.; Stadermann, M.; Artyukhin, A. B.; Grigoropoulos, C. P.; Noy, A.; Bakajin, O. Fast Mass Transport through Sub-2-Nanometer Carbon Nanotubes. *Science* **2006**, *312*, 1034−1037.

(2) Hinds, B. J.; Chopra, N.; Rantell, T.; Andrews, R.; Gavalas, V.; Bachas, L. G. Aligned Multiwalled Carbon Nanotube Membranes. *Science* **2004**, *303*, 62−65.

(3) Majumder, M.; Keis, K.; Zhan, X.; Meadows, C.; Cole, J.; Hinds, B. J. Enhanced Electrostatic Modulation of Ionic Diffusion through Carbon Nanotube Membranes by Diazonium Grafting Chemistry. *J. Membr. Sci.* **2008**, *316*, 89−96.

(4) Fornasiero, F.; Park, H. G.; Holt, J. K.; Stadermann, M.; Grigoropoulos, C. P.; Noy, A.; Bakajin, O. Ion Exclusion by Sub-2-Nm Carbon Nanotube Pores. *Proc. Natl. Acad. Sci. U. S. A.* **2008**, *105*, 17250−17255.

(5) Sun, X.; Su, X.; Wu, J.; Hinds, B. J. Electrophoretic Transport of Biomolecules through Carbon Nanotube Membranes. *Langmuir* **2011**, *27*, 3150−3156.

(6) Wu, J.; Gerstandt, K.; Zhang, H.; Liu, J.; Hinds, B. J. Electrophoretically Induced Aqueous Flow through Single-Walled Carbon Nanotube Membranes. *Nat. Nanotechnol.* **2012**, *7*, 133−139.

(7) Wu, J.; Paudel, K. S.; Strasinger, C.; Hammell, D.; Stinchcomb, A. L.; Hinds, B. J. Programmable Transdermal Drug Delivery of Nicotine Using Carbon Nanotube Membranes. *Proc. Natl. Acad. Sci. U. S. A.* **2010**, *107*, 11698−11702.

(8) Futaba, D. N.; Hata, K.; Namai, T.; Yamada, T.; Mizuno, K.; Hayamizu, Y.; Yumura, M.; Iijima, S. 84% Catalyst Activity of Water-Assisted Growth of Single Walled Carbon Nanotube Forest Characterization by a Statistical and Macroscopic Approach. *J. Phys. Chem. B* **2006**, *110*, 8035−8038.

(9) Sakurai, S.; Inaguma, M.; Futaba, D. N.; Yumura, M.; Hata, K. Diameter and Density Control of Single-Walled Carbon Nanotube Forests by Modulating Ostwald Ripening through Decoupling the Catalyst Formation and Growth Processes. *Small* **2013**, *21*, 3584−3592.

(10) Zhong, G.; Warner, J. H.; Fouquet, M.; Robertson, A. W.; Chen, B.; Robertson, J. Growth of Ultrahigh Density Single-Walled Carbon Nanotube Forests by Improved Catalyst Design. *ACS Nano* **2012**, *6*, 2893−2903.

(11) Jiang, K.; Wang, J.; Li, Q.; Liu, L.; Liu, C.; Fan, S. Superaligned Carbon Nanotube Arrays, Films, and Yarns: A Road to Applications. *Adv. Mater.* **2011**, *23*, 1154−1161.

(12) Hata, K.; Futaba, D. N.; Mizuno, K.; Namai, T.; Yumura, M.; Iijima, S. Water-Assisted Highly Efficient Synthesis of Impurity-Free Single-Walled Carbon Nanotubes. *Science* **2004**, *306*, 1362−1364.

(13) Sakurai, S.; Nishino, H.; Futaba, D. N.; Yasuda, S.; Yamada, T.; Maigne, A.; Matsuo, Y.; Nakamura, E.; Yumura, M.; Hata, K. Role of Subsurface Diffusion and Ostwald Ripening in Catalyst Formation for Single-Walled Carbon Nanotube Forest Growth. *J. Am. Chem. Soc.* **2012**, *134*, 2148−2153.

(14) In, J. B.; Grigoropoulos, C. P.; Chernov, A. A.; Noy, A. Hidden Role of Trace Gas Impurities in Chemical Vapor Deposition Growth of Vertically-Aligned Carbon Nanotube Arrays. *Appl. Phys. Lett.* **2011**, *98*, 153102−153102-3.

(15) Seah, C.-M.; Chai, S.-P.; Mohamed, A. R. Synthesis of Aligned Carbon Nanotubes. *Carbon* **2011**, *49*, 4613−4635.

(16) Zhang, G.; Mann, D.; Zhang, L.; Javey, A.; Li, Y.; Yenilmez, E.; Wang, Q.; McVittie, J. P.; Nishi, Y.; Gibbons, J. Ultra-High-Yield Growth of Vertical Single-Walled Carbon Nanotubes: Hidden Roles of Hydrogen and Oxygen. *Proc. Natl. Acad. Sci. U. S. A.* **2005**, *102*, 16141−16145.

(17) Hasegawa, K.; Noda, S. Millimeter-Tall Single-Walled Carbon Nanotubes Rapidly Grown with and without Water. *ACS Nano* **2011**, *5*, 975−984.

(18) Nessim, G. D.; Al-Obeidi, A.; Grisaru, H.; Polsen, E. S.; Ryan Oliver, C.; Zimrin, T.; John Hart, A.; Aurbach, D.; Thompson, C. V. Synthesis of Tall Carpets of Vertically Aligned Carbon Nanotubes by in Situ Generation of Water Vapor through Preheating of Added Oxygen. *Carbon* **2012**, *50*, 4002−4009.

(19) Yang, X.; Yuan, L.; Peterson, V. K.; Yin, Y.; Minett, A. I.; Harris, A. T. Open-Ended Aligned Carbon Nanotube Arrays Produced Using CO_2-Assisted Floating-Ferrocene Chemical Vapor Deposition. *J. Phys. Chem. C* **2011**, *115*, 14093−14097.

(20) Huang, J.; Zhang, Q.; Zhao, M.; Wei, F. Process Intensification by CO_2 for High Quality Carbon Nanotube Forest Growth: Double-

Walled Carbon Nanotube Convexity or Single-Walled Carbon Nanotube Bowls? *Nano Res.* **2009**, *2*, 872−881.
(21) Futaba, D. N.; Goto, J.; Yasuda, S.; Yamada, T.; Yumura, M.; Hata, K. General Rules Governing the Highly Efficient Growth of Carbon Nanotubes. *Adv. Mater.* **2009**, *21*, 4811−4815.
(22) Amama, P. B.; Pint, C. L.; McJilton, L.; Kim, S. M.; Stach, E. A.; Murray, P. T.; Hauge, R. H.; Maruyama, B. Role of Water in Super Growth of Single-Walled Carbon Nanotube Carpets. *Nano Lett.* **2008**, *9*, 44−49.
(23) Hasegawa, K.; Noda, S. Moderating Carbon Supply and Suppressing Ostwald Ripening of Catalyst Particles to Produce 4.5-mm-Tall Single-Walled Carbon Nanotube Forests. *Carbon* **2011**, *49*, 4497−4504.
(24) Rosenfeld, G.; Morgenstern, K.; Esser, M.; Comsa, G. Dynamics and Stability of Nanostructures on Metal Surfaces. *Appl. Phys. A: Mater. Sci. Process.* **1999**, *69*, 489−496.
(25) Fotiadis, D. I.; Kieda, S.; Jensen, K. F. Transport Phenomena in Vertical Reactors for Metalorganic Vapor Phase Epitaxy: I. Effects of Heat Transfer Characteristics, Reactor Geometry, and Operating Conditions. *J. Cryst. Growth* **1990**, *102*, 441−470.
(26) Kaneko, A.; Yamada, K.; Kumahara, R.; Kato, H.; Homma, Y. Comparative Study of Catalytic Activity of Iron and Cobalt for Growing Carbon Nanotubes on Alumina and Silicon Oxide. *J. Phys. Chem. C* **2012**, *116*, 26060−26065.
(27) Nagashima, K.; Yanagida, T.; Oka, K.; Tanaka, H.; Kawai, T. Mechanism and Control of Sidewall Growth and Catalyst Diffusion on Oxide Nanowire Vapor-Liquid-Solid Growth. *Appl. Phys. Lett.* **2008**, *93*, 153103.
(28) Kodambaka, S.; Hannon, J. B.; Tromp, R. M.; Ross, F. M. Control of Si Nanowire Growth by Oxygen. *Nano Lett.* **2006**, *6*, 1292−1296.
(29) Hannon, J. B.; Kodambaka, S.; Ross, F. M.; Tromp, R. M. The Influence of the Surface Migration of Gold on the Growth of Silicon Nanowires. *Nature* **2006**, *440*, 69−71.
(30) Youn, S. K.; Yazdani, N.; Patscheider, J.; Park, H. G. Facile Diameter Control of Vertically Aligned, Narrow Single-Walled Carbon Nanotubes. *RSC Adv.* **2013**, *3*, 1434−1441.
(31) Saunders, S. R. J.; Monteiro, M.; Rizzo, F. The Oxidation Behaviour of Metals and Alloys at High Temperatures in Atmospheres Containing Water Vapour: A Review. *Prog. Mater. Sci.* **2008**, *53*, 775−837.
(32) de los Arcos, T.; Garnier, M. G.; Seo, J. W.; Oelhafen, P.; Thommen, V.; Mathys, D. The Influence of Catalyst Chemical State and Morphology on Carbon Nanotube Growth. *J. Phys. Chem. B* **2004**, *108*, 7728−7734.
(33) Amama, P. B.; Pint, C. L.; Mirri, F.; Pasquali, M.; Hauge, R. H.; Maruyama, B. Catalyst−Support Interactions and Their Influence in Water-Assisted Carbon Nanotube Carpet Growth. *Carbon* **2012**, *50*, 2396−2406.
(34) Teblum, E.; Gofer, Y.; Pint, C. L.; Nessim, G. D. Role of Catalyst Oxidation State in the Growth of Vertically Aligned Carbon Nanotubes. *J. Phys. Chem. C* **2012**, *116*, 24522−24528.
(35) Mattevi, C.; Wirth, C. T.; Hofmann, S.; Blume, R.; Cantoro, M.; Ducati, C.; Cepek, C.; Knop-Gericke, A.; Milne, S.; Castellarin-Cudia, C. In-Situ X-ray Photoelectron Spectroscopy Study of Catalyst—Support Interactions and Growth of Carbon Nanotube Forests. *J. Phys. Chem. C* **2008**, *112*, 12207−12213.